Proceedings World Geothermal Congress 2020+1
Reykjavik, Iceland, April - October 2021

Influence of Precipitating Brine Components on Materials Selection for Geothermal Applications

Anastasia Stoljarova[1], Ralph Bäßler[2], Simona Regenspurg[3]

[1] Freie Universität Berlin, Institute for Chemistry and Biochemistry, Takustraße 3, D-14195 Berlin/Germany

[2] BAM – Bundesanstalt für Materialforschung und -prüfung, Unter den Eichen 87, D-12205 Berlin/Germany

[3] GFZ - German Research Centre for Geosciences, Telegrafenberg, D-14473 Potsdam/Germany

[1] An.St@FU-Berlin.de, [2] Ralph.Baessler@BAM.de, [3] Regens@GFZ-Potsdam.de

Keywords: copper, lead, corrosion, steel, geothermal energy

ABSTRACT

Since geothermal wells are a feasible energy source to replace fossil fuel supply, many technologies have been developed to take advantage of geothermal energy. Nevertheless, service conditions in geothermal facilities are in many cases extreme in terms of corrosion due to the chemical composition of hydrothermal fluids and temperatures. Therefore, materials selection based on preliminary material qualification is essential to guarantee a secure and reliable operation of the facilities. During operation of a geothermal research facility in Groß Schönebeck copper and lead effects have been found downhole. Occurring mechanisms and measures to prevent precipitation or scaling needed to be investigated as well as potential influences of such precipitates on corrosion resistance of metallic materials used for equipment.

This contribution deals with the evaluation of the corrosion behavior of carbon steel and corrosion resistant alloys in copper and/or lead containing artificial geothermal water, simulating the conditions in the Northern German Basin.

The behavior of these materials in an artificial geothermal water obtained by electrochemical measurements and exposure tests are presented. While carbon steel exhibits precipitation and deposition, higher alloyed material shows different response to such species and a higher resistance in saline geothermal water.

Basing on these results the suitability of the investigated corrosion resistant alloy is given for use in such conditions, whereas carbon steel creates difficulties due to its susceptibility to Cu- and Pb-precipitation.

1 INTRODUCTION

Since geothermal reservoirs are a feasible energy source to replace fossil fuel supply, many technologies have been developed to take advantage of geothermal energy. Nevertheless, due to the chemical composition of hydrothermal fluids and temperatures, service conditions in geothermal facilities are demanding in many cases in terms of corrosion. Therefore, materials selection based on preliminary material qualification is essential to guarantee a secure and reliable operation of the facilities [1].

Since operational conditions in geothermal power plants are crucial in terms of corrosion special attention is paid to materials selection [2 - 5].

During fluid circulation test at the geothermal research facility Groß Schönebeck (Germany), massive copper precipitation has been observed downhole in 4200 m depth, clogging the production well and reducing the productivity. Presumably Cu forms directly in the borehole by reduction of dissolved Cu^{2+} by oxidation of iron from the steel casing [6 - 8], leading to clogging of reservoir pores in the well bore-near area and galvanic copper deposition on equipment and piping [9]. Preliminary laboratory tests also pointed to a potential similar danger, caused by lead components [3].

In order to evaluate the corrosion behavior of different metals, exposure and electrochemical tests were performed in artificial geothermal water, simulating the conditions of formation water in the Rotliegend formation in the Northern German Basin (highly saline, about 150 °C), especially regarding the effect of copper and lead content.

Beside the already high corrosivity of the geothermal brine due to the high saline content, copper and lead deposition are dominating reactions determining the suitability of materials used. Such reactions only occur when carbon steel is involved.

2 EXPERIMENTAL SETUP

2.1 Materials and Conditions

The corrosion resistance of carbon steel and Ni-rich corrosion resistant alloys (CRA) and their influence on the copper resp. lead reduction was investigated by exposure and electrochemical tests in artificial saline water at 150 °C, simulating downhole conditions. In terms of high alloyed stainless steel, Cu related investigations were performed on alloy 904L. Pb involved tests were conducted on alloy 31. The composition of materials used are shown in Table 1.

Beside these materials different stainless steels were investigated as well in terms of copper effect. Results were already presented elsewhere [16].

For the measurements, the oxygen concentration in the water was adjusted to very low values by purging the solution with argon for 10 min prior to start of measurements. The test pressure of 1500 kPa was achieved using argon pre-pressurization. The medium was not stirred or purged during exposure.

Test solution was an artificial saline water with a composition comparable to a reference analysis of geothermal fluids found in Groß Schönebeck [3], consisting of an aqueous solution with 2 mol/L NaCl and 1.5 mol/L ($CaCl_2 \cdot 2\ H_2O$). For investigations presented here, 63 mg/L Cu^{2+} (as $CuSO_4$) resp. 20 mg/L Pb^{2+} (as $PbCl_2$) were added.

Table 1: Chemical Composition according manufacturer's datasheets [10 - 13]

		Content [mass%]								
		Cr	**Ni**	**Mo**	**Fe**	**Mn**	**C**	**N**	**Cu**	**Si**
Carbon Steel	**S235JR** (ST 37-2, 1.0038)	-	-	-	R	≤ 1.4	≤ 0.2	-	-	-
CRA	**X1NiCrMoCu25-20-5** (904L, N08904, 1.4539)	19 - 21	24 - 26	4 - 5	R	≤ 2	≤ 0.02	≤ 0.15	1.2 - 2	≤ 0.7
	X1NiCrMoCu32-28-7 (alloy 31, N08091, 1.4562)	26 - 28	30 - 32	6 - 7	R	≤ 2	≤ 0.015	0.15 – 0.25	1 – 1.4	≤ 0.3

2.2 Exposure Tests

Exposure tests were carried out according to DIN 50905/4 [14] with gravimetric determination of time dependent corrosion within a heating cabinet to provide uniform temperature distribution [15]. Tests were carried out in 1-Liter-autoclaves (figure 1) having a glass-inlay. Three specimens were completely immersed into the solution. Exposure time was up to one month at 150 °C.

Copper deposition was determined after 1 day and one week. Lead effect was determined after 7 and 30 days.

Figure 1: Vessels for exposure tests

Test specimens were machined from a plate by water jetting. Before testing, surfaces were ground by 120 SiC-paper, degreased by acetone and dried. The size for test specimens (l x w x t) was 20 x 7 x 6 mm. A set of 3 specimens was used. Each exposure test specimen had a 5 mm hole for fixation using a polytetrafluoroethylene (PTFE)-cord (figure 2, left).

To prevent interaction between the different materials and their corrosion products, the specimens were placed in glass beakers inside the autoclave and tested separately for each material. The specimens were completely immersed in the water. The threshold for suitability was set to be a corrosion rate of 0.1 mm/year. This corresponds to a wall thickness reduction of 2 mm by uniform corrosion during 20 years of service.

Figure 2: Specimen design for exposure (left) and electrochemical (right) tests

Beside the determination of weight loss, localized corrosion phenomena were investigated on the gravimetric specimens as well.

A distinction was drawn between pitting and shallow pit corrosion to use the right criteria for the suitability assessment. This means when pitting occurs, the material is not suitable. In case of shallow pitting the depth of the shallow pit was extrapolated to one year resulting in the corrosion rate. Specimens were evaluated after the tests using optical microscopy.

2.3 Electrochemical Tests

For electrochemical characterization free corrosion potentials (E_{cor}) were recorded for 1 to 10 days. Afterwards current density potential curves (CPC) were recorded starting at -200 mV relative to E_{cor} and proceeded in the anodic direction with 0.2 mV/s linear sweep rate. As soon as the potential was 1.2 V higher than E_{cor} or the max. allowed current density i_{cor} excided 25 mA/cm² for C-steel, resp. 1 mA/cm² for CRA, the scan was reversed in the cathodic direction, back to -200 mV vs. E_{cor}. The critical potential, E_{crit} and the repassivation potential E_{rep}, were determined at i_{cor} = 0.1 mA/cm². Before immersion of test specimens, the solution was purged by argon to keep the oxygen-content very low.

Investigations were carried out using a typical 3-electrode configuration within a 1-L-autoclave equipped with a PTFE-encapsulated saturated Ag/AgCl reference electrode (-220 mV_{SHE}) and a Ti-oxide covered titanium mesh as a counter electrode. The temperature in the autoclave was adjusted by an external hotplate and constantly monitored by a thermocouple. An uniform heat distribution was provided by an Al-jacked around the autoclave body (figure 3). The specimen size for electrochemical tests resulted in 8 cm² surface (figure 2, right). All specimens were ground to grit 320 to have comparable surface conditions.

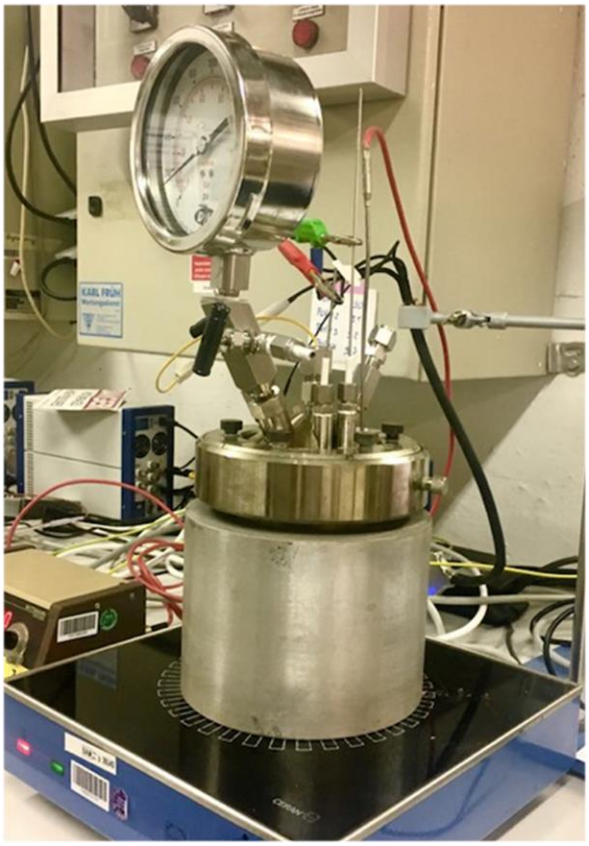

Figure 3: Test setup for electrochemical tests

3 RESULTS

3.1 Exposure Tests

3.1.1 Cu-deposition [16]

Already after 24 hours a uniformly distributed copper layer was found on carbon steel. Appearance of specimen surface and thickness of deposited Cu-layer are shown in figure 4. After one day a thickness of 4.53 µm was determined growing to 14.75 µm after one week.

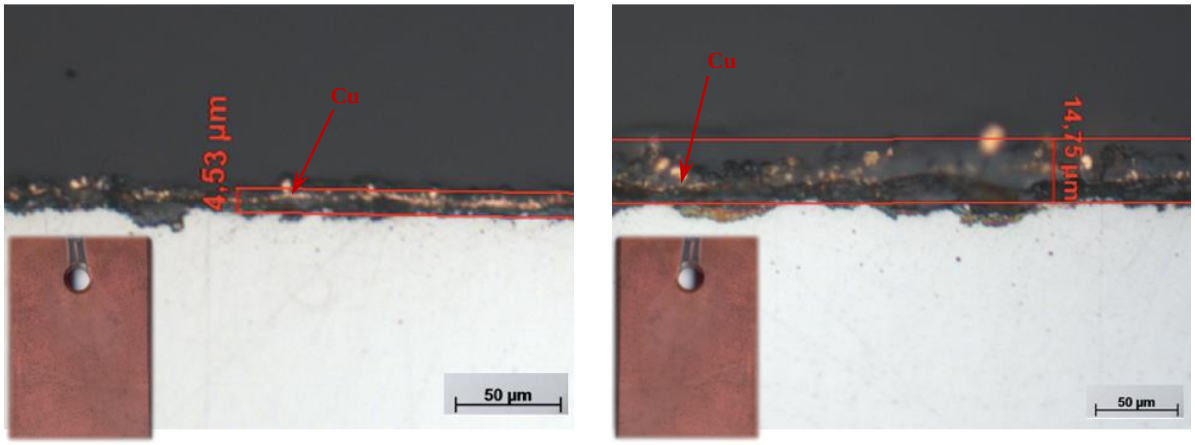

Figure 4: Copper deposition on carbon steel after 1 day (left) and 1 week (right)

Additionally, the copper concentration of the medium was measured. At the beginning it was 63 mg/L, after 24 hours 9.5 mg/L and after one week 5.4 mg/L. So continuous deposition could be observed. Also, a reddish precipitation (presumably Cu and iron hydroxide) was detected.

Exposure tests with CRA did not show detectable copper depositions. Much less precipitation could be detected. The copper content of the solution decreased from 63 mg/L to 54.3 mg/L after one week and 48 mg/L after one month. Appearance of the CRA test specimens after certain times of exposure in Cu-containing artificial geothermal water is shown in figure 5. In addition to no Cu-deposition, no signs of general or pitting corrosion could be detected. Within the area of fixation some markups pointed to a potential susceptibility to crevice corrosion, as discussed already in previous publications [2 - 5].

1 week 1 month

Figure 5: Surface appearance of CRA after one week and 30 days exposure in Cu-containing geothermal water

3.1.2 Pb-deposition

Specimens exposed to Pb containing solution showed Pb-deposition on C-steel but not on CRA (figures 6 and 7).

Similar results were obtained on specimens exposed to the solution containing both Cu and Pb (figure 8). Here a domination of Cu-deposition is assumed (clearly visible at 30 d-specimen). Slightly reddish coloration of the specimens exposed in Pb/Cu-solution point to Cu deposited on the surface. Cross sections clearly showed Cu-species on top of C-steel, but none on the CRA (figure 9). Pb stuck to the specimen's surface only loosely, as non-magnetic particles found in the solution suggest (figure 10).

In addition to deposition and corrosion effects signs of crevice corrosion susceptibility and deposition disturbance were found at C-steel specimens within the area of fixation (figures 4, 6 and 8; left).

Figure 6: Specimens after 7, 30 and 100 days in Pb-containing solution at 150 °C

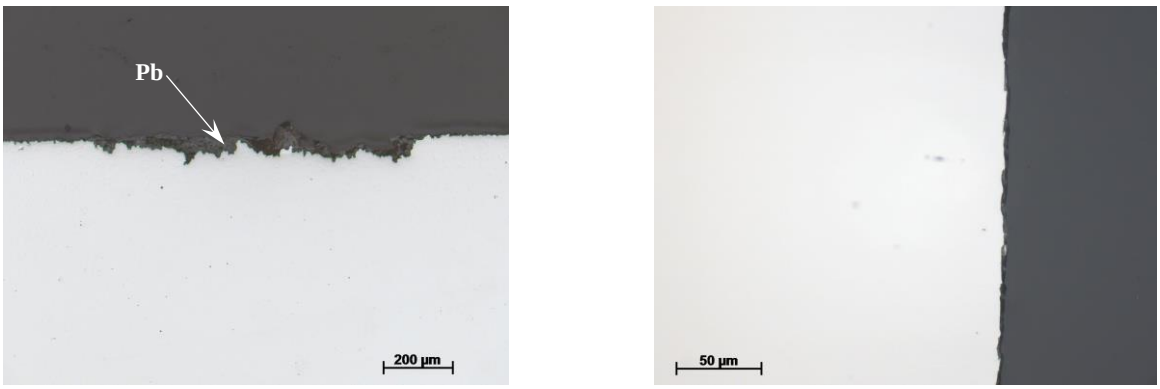

Figure 7: Cross sections after 7 d exposure of C-steel (left) and CRA (right) in Pb-solution at 150 °C

Figure 8: Specimens after 7, 30 and 100 days in Pb/Cu-containing solution at 150 °C

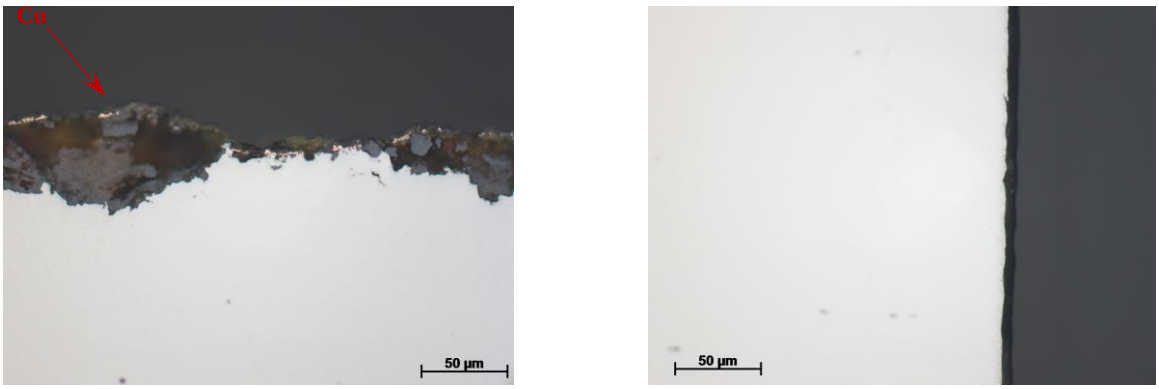

Figure 9: Cross sections after 7 d exposure of C-steel (left) and CRA (right) in Pb/Cu-solution at 150 °C

Figure 10: Appearance after 100 d exposure of C-steel in Pb- (left) and Pb/Cu- (right) solution at 150 °C with precipitations filtered from the solution

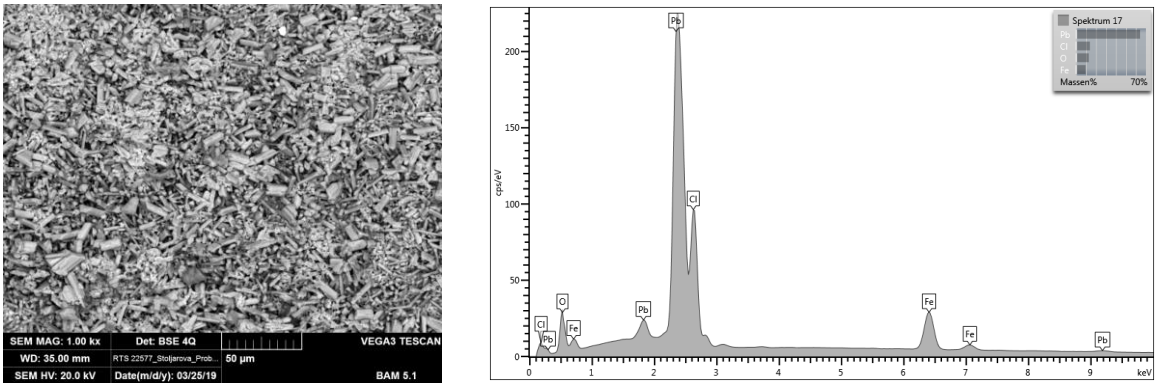

Figure 11: EDX spectrum on C-steel after 30 days exposure in Pb-solution at 150 °C

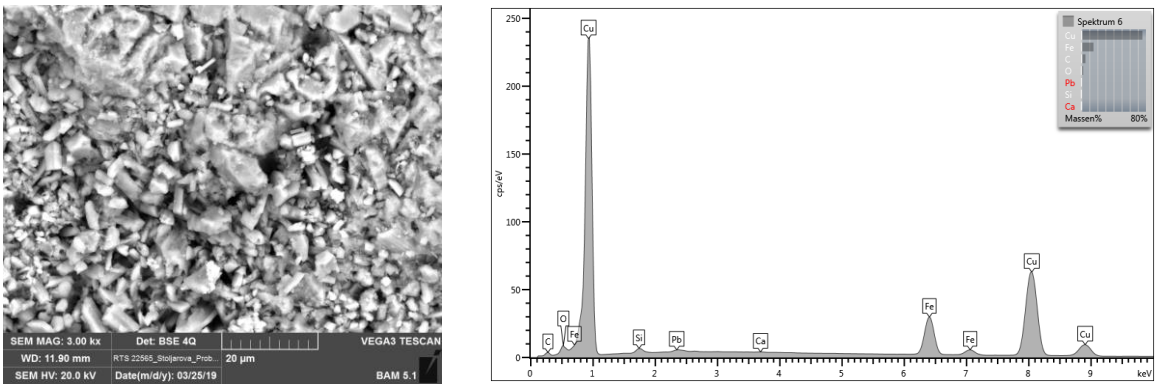

Figure 12: EDX spectrum on C-steel after 30 days exposure in Pb/Cu-solution at 150 °C

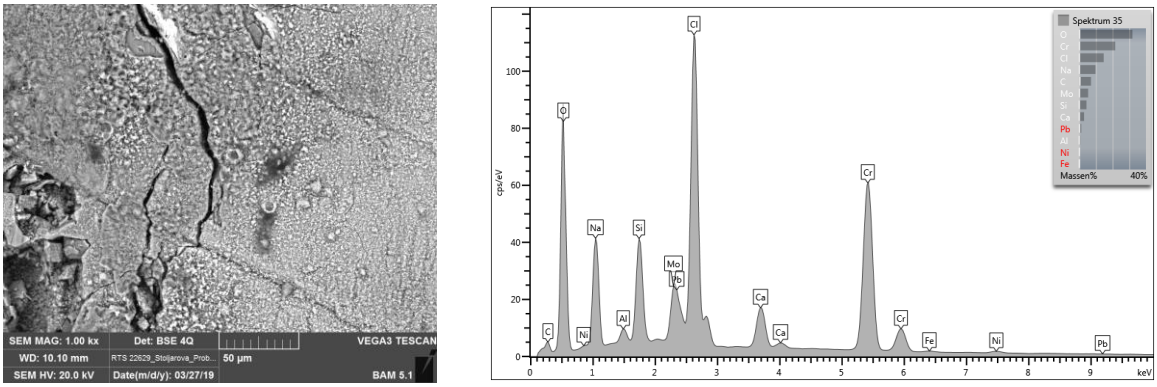

Figure 13: EDX spectrum on CRA after 30 days exposure in Pb/Cu-solution at 150 °C

EDX-analysis of C-steel surface after 30 days exposure in Pb-solution showed deposited Pb (figure 11). In case of exposure in Pb/Cu-solution Cu-domination and some hints to Pb could be observed (figure 12). No Cu, but just a slight hint to Pb could be detected on CRA exposed in Pb/Cu-solution (figure 13). No Cu-species could be detected.

3.2 Electrochemical Tests

3.2.1 Free Corrosion Potential

All specimens exhibited quite stable free corrosion potentials (E_{cor}) after reaching the desired test temperature (figure 14). Previous experiments reveal that they remain stable, even for exposures over 6 months [3].

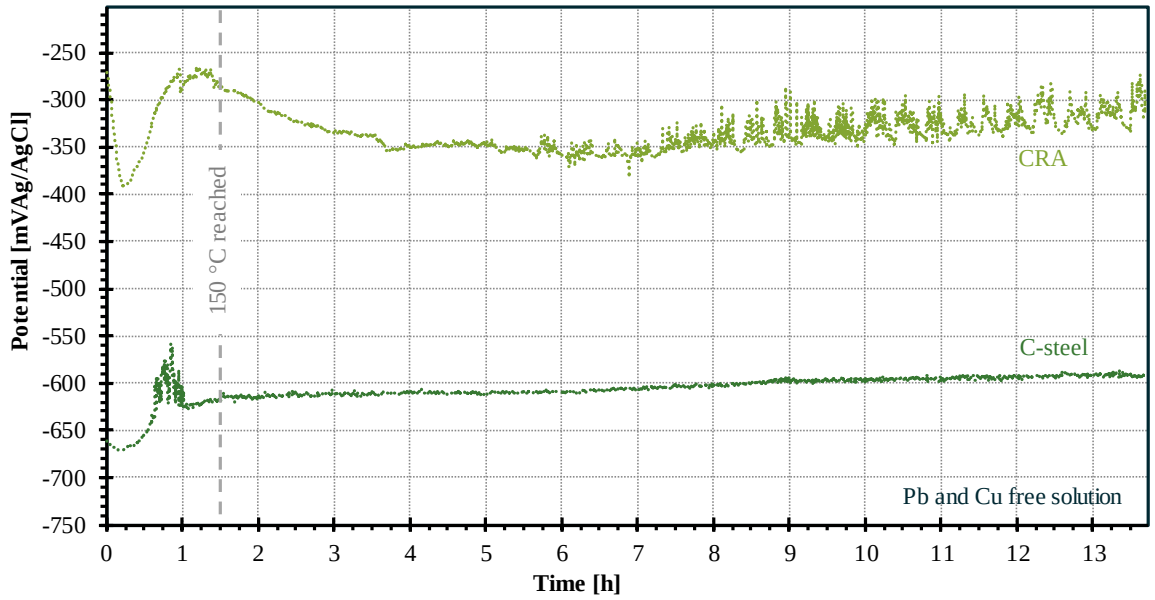

Figure 14: Free corrosion potentials on C-steel and CRA in artificial Cu- and Pb-free geothermal water

Selected recorded potentials after reaching the test temperature are shown in figure 15. A survey of measured values is given in table 2. As expected, E_{cor} of C-steel was lower than that of CRA.

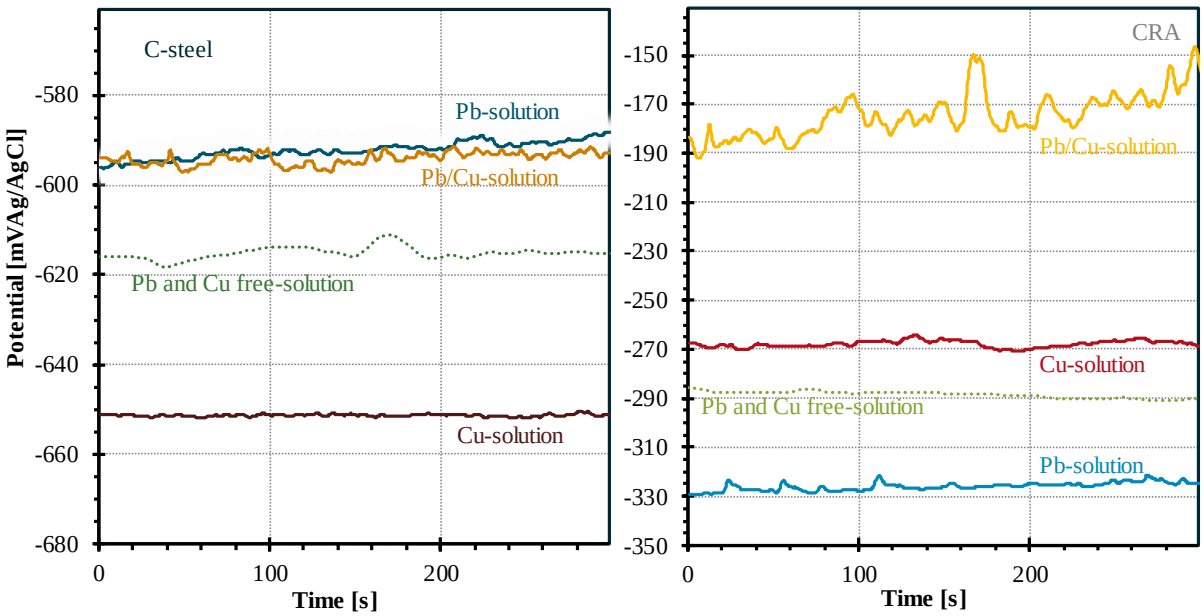

Figure 15: Free corrosion potentials in various artificial geothermal waters (left: C-steel; right: CRA)

3.2.2 Current Density Potential Curves

Current density potential curves measured at different materials are shown in figure 16. A significant difference was found, following the E_{cor} ranking.

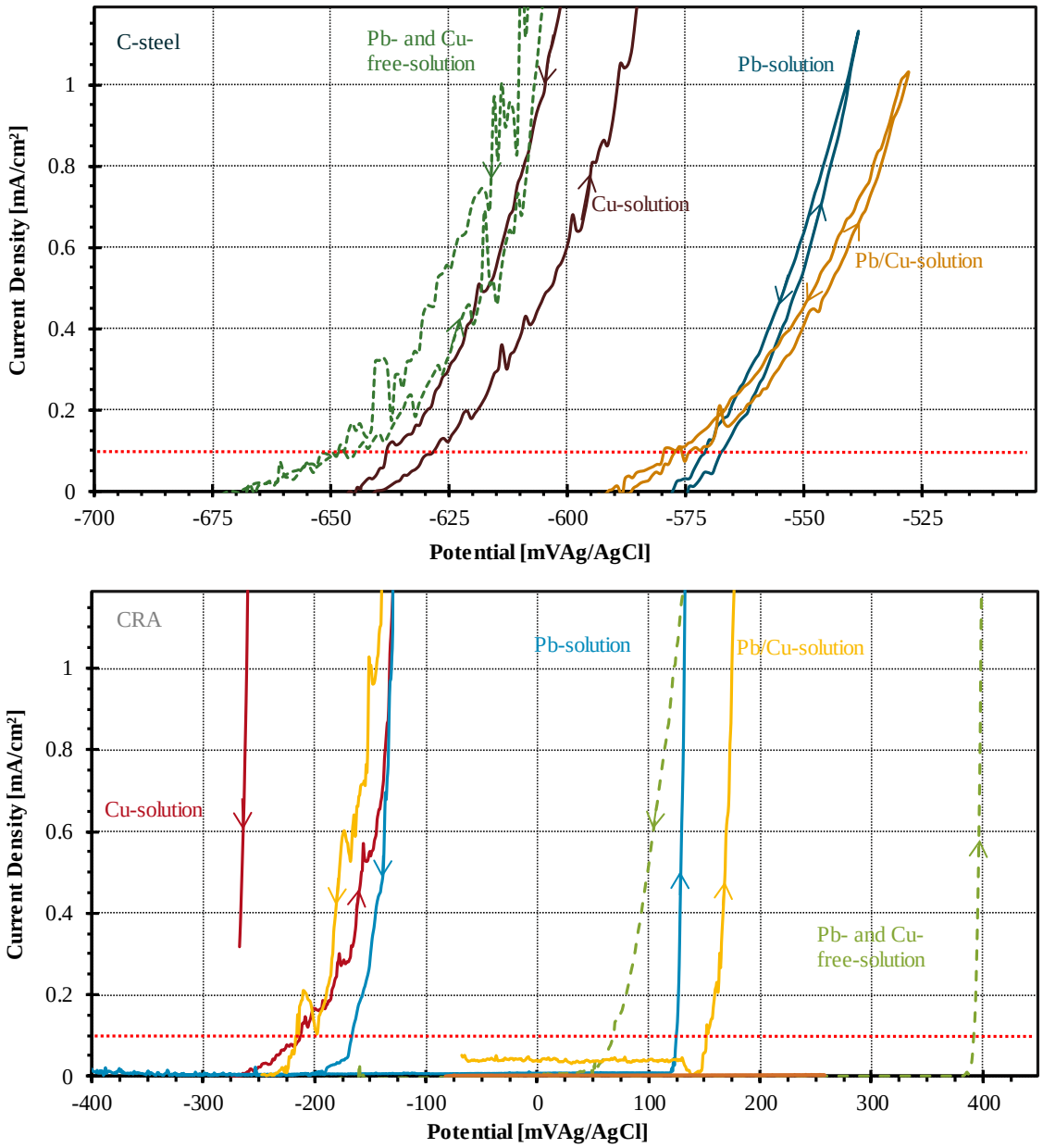

Figure 16: Current density potential curves in various artificial geothermal waters (top: C-steel; below: CRA)

Polarizing the specimens caused Cu deposition on C-steel. Hysteresis (pointing to localized corrosion and bad repassivation behavior) could be found for the CRA. Surface appearance is shown in figure 17.

.

Figure 17: C-steel (left) and CRA (right) specimens after cyclic polarization in Cu-, Pb- and Pb/Cu-containing solution at 150 °C

The crevice effect, seen in the fixation areas during exposure tests was not investigated furthermore, since this effect has been described in previous publications [2 - 5, 17].

4 EVALUATION

In table 2 results of electrochemical tests are summarized. The last column contains the evaluation resulting from comparison of free corrosion and critical potentials. As already described above, critical potentials of C-steel were determined being close to the E_{cor}, indicating corrosion susceptibility. For C-steel Cu-deposition process is dominant. At CRA the critical corrosion potential is far away from free corrosion potential. So, no corrosion susceptibility would be expected. However, the repassivation potential in Cu-containing solution is close to the E_{cor}, indicating a bad repassivation behavior. Hence, once corrosion has started due to changes in the system, these materials might not become passive again. Lead in the solution would make the repassivation behavior better.

Table 2: Critical potentials from electrochemical measurements (150 °C)

	E_{cor} [$mV_{Ag/AgCl}$]	E_{crit} [$mV_{Ag/AgCl}$]	E_{rep} [$mV_{Ag/AgCl}$]	status at E_{cor}
Cu-containing medium				
C-steel	-651 ± 6	-604 ± 42	-589 ± 61	active
CRA	-269 ± 2	-132 ± 52	-261 ± 11	passive
Pb-containing medium				
C-steel	-580 ± 40	-585 ± 43	-567 ± 34	active
CRA	-310± 3	125 ± 5	-167 ± 62	passive
Cu and Pb-containing medium				
C-steel	-590 ± 2	-580 ± 2	-577 ± 4	active
CRA	-189 ± 70	152 ± 55	70 ± 85	passive
Cu and Pb-free medium				
C-steel	-674 ± 10	-650 ± 10	-649 ± 10	active
CRA	-74 ± 12	391 ± 10	69 ± 10	passive

5 CONCLUSIONS

By exposure and electrochemical tests in the laboratory the Cu- and Pb-effect on corrosion behavior and performance of carbon steel and a corrosion resistant alloy could be assessed. Critical material specific properties were determined by static exposure and electrochemical tests in artificial geothermal water with high salinity and low pH, containing Cu/Pb.

It could be shown that significant Cu- resp. Pb-deposition and -precipitation only occurred in combination with carbon steel. Corrosion resistant alloys (e. g. Cr- and Ni-dominated stainless steels) prevent the disturbing Cu-agglomeration resp. Pb-deposition. Therefore, they are suitable to be chosen for future design of geothermal piping system, either in massive or in cladded form. Regarding corrosion, formation of crevices with non-metallic materials shall be avoided.

So, in addition to its already known limited corrosion resistance, carbon steel shall not be used when copper or lead species are content of the geothermal brine. Otherwise precipitation and/or deposition of metallic copper resp. lead must be expected, increasing the susceptibility of clogging the piping system.

From the interactions and pitting corrosion point of view, corrosion resistant alloys (preferably Ni-rich) seem to be most favorable when selecting materials for applications in such geothermal brines.

OUTLOOK

Publication of results achieved so far will contribute to a materials selection for a new well to be drilled for re-activating Groß Schönebeck research facility or other facilities facing similar aquifer fluid situations.

ACKNOWLEDGEMENT

Materials were provided by Butting and VDM-Metals. This work was financially supported by the German Ministry of Economics and Energy (BMWi) on the grant number 0324065.

The authors thank for the support.

REFERENCES

[1] R. Bäßler: Assessment of Metallic Materials for Geothermal Applications, World Geothermal Congress 2010, Bali

[2] R. Bäßler, A. Burkert, R. Kirchheiner, A. Saadat, M. Finke: Evaluation of Corrosion Resistance of Materials for Geothermal Applications, NACE International Conference, Corrosion 2009, New Orleans, USA, paper 09377

[3] R. Bäßler, J. Sobetzki, H. Sarmiento Klapper: Corrosion Resistance of High-Alloyed Materials in Artificial Geothermal Brines, European Geothermal Congress 2013, Pisa, Italy, paper HS4-27

[4] A. Keserović, R. Bäßler: Materials Evaluation for Geothermal Applications in Different Geothermal Waters, Proceedings World Geothermal Congress 2015, Melbourne, paper 27011

[5] H. Sarmiento Klapper, R. Bäßler, A. Saadat, H. Asteman: Evaluation of Suitability of Some High-Alloyed Materials for Geothermal Applications, NACE International Conference, Corrosion 2011, Houston, USA, paper 11172

[6] S. Regenspurg, E. Feldbusch, A. Saadat: Corrosion processes at the geothermal site Groß Schönebeck (North German Basin), NACE International Corrosion Conference 2013, Orlando, USA, paper 2606

[7] S. Regenspurg, E. Feldbusch, J. Byrne, F. Deon, D. L. Driba, J. Henninges, A. Kappler, R. Naumann, T. Reinsch, C. Schubert: Mineral precipitation during production of geothermal fluid from a Permian Rotliegend reservoir, Geothermics 54, 2015, p. 122 - 135

[8] S. Regenspurg, I. Geigenmüller, H. Milsch and M. Kühn: Copper precipitation as consequence of steel corrosion in a flow-through experiment mimicking a geothermal production well, Geotherm Energy (2017) 5:11, DOI 10.1186/s40517-017-0069-9

[9] T. Reinsch, S. Kranz, A. Saadat, E. Huenges, M. Rinke, W. Brandt, P. Schulz: Balanced Reverse-Cleanout Operation: Removing Large and Heavy Particles from a Geothermal Well, J. Society of Petroleum Engineers Production & Operations, Vol. 32, Issue 3, 2017

[10] Thyssen-Krupp, Produktinformationen precidur, 2018

[11] Butting - Werkstofftabellen, 2017

[12] VDM-Metals, Materials-Data-Sheet “alloy 31” 2019

[13] Timet, Materials-Data-Sheet “Grade 2”, 2015

[14] Deutsches Institut für Normung (DIN): German Standard DIN 50905/4: “Corrosion of metals; corrosion testing; corrosion testing in liquids under laboratory conditions without mechanical stress”, 1987

[15] R. Bäßler: Evaluation of Metallic Materials for Geothermal Applications, European Geothermal Congress 2016, Strasbourg, France, paper T-HP-248

[16] A. Stoljarova, R. Bäßler, S. Regenspurg: Material qualification in saline, copper containing geothermal water, NACE International Conference, Corrosion 2019, Nashville, USA, paper 12862

[17] A. Keserović, R. Bäßler, Y. Kamah: Suitability of alloyed steels in highly acidic environments, NACE International Conference, Corrosion 2014, San Antonio, USA, paper 4031